17th Brazilian Congress of Thermal Sciences and Engineering
November 25th-28th, 2018, Águas de Lindóia, SP, Brazil

ENCIT-2018-0080
APPLICATION OF WAF-TVD SCHEME FOR WATER HAMMER EQUATIONS

Raphael C. Carvalho
Helcio R. B. Orlande
Marcelo J. Colaço
Federal University of Rio de Janiero, Departament of Mechanical Engineering/DEM-PEM/COPPE-UFRJ
Athos da Silveira Ramos Avenue 149, 21941-909, Cidade Universitária, Rio de Janeiro, Brazil
raphael.costa.carvalho@poli.ufrj.br
helcio@mecanica.coppe.ufrj.br
colaco@ mecanica.coppe.ufrj.br

Italo Márcio Madeira
Petrobras – Petróleo Brasileiro S.A.. CENPES- Petrobras Research and Development Center.
Horácio de Macedo Avenue 950, 21941-915 – Cidade Universitária, Rio de Janeiro, Brazil
italomadeira@petrobras.com.br

Abstract. *Non-stationary flows have great importance for many engineering problems. Whenever the velocity of the flow in a pipe changes rapidly, pressures waves are generated inside the ducts in a phenomenon called water hammer or hydraulic transient. The consequences of this process can be very dangerous to the hydraulic system integrity. Therefore, it is important to understand how the pressure waves behave in such situations, through numerical and experimental simulations of different scenarios. The present work aims at the numerical solution of the water hammer problem in straight pipes. The hydraulic transient equations are solved through the finite volume method, using a TVD (Total Variation Diminishing) version of the WAF (Weighted Average Flux) scheme. The numerical code developed in this work is verified and validated with data available in the literature.*

Keywords: *Water Hammer, WAF-TVD, Numerical Method.*

1. INTRODUCTION

Water hammer occurs when there is a rapid change in the flow velocity in a pipe. This change may occur as a response to a sudden closure of a gate valve, a sudden failure in the system or a pump trip (Lüdeck and Kothe, 2006). Due to the fluid inertia, the liquid phase velocity is not capable of adjusting itself to the new flow regime. As a result, part of the kinetic energy of the fluid turns into pressure energy, generating pressure waves inside the duct, which compress the liquid and deform the pipe walls.

The pressure waves in the water hammer can severely affect the hydraulic system. Due to its high magnitude and wave speeds (around 1000 m/s), they can even cause plastic deformation of the ducts and structural failures of the pipe and its accessories (Boulos *et al*., 2005). Another problem refers to vibrations. Strong hydraulic vibrations can arise in response to the pressure waves, damaging the supports of the pipelines and inducing fatigue failures (if these vibrations occur during an extended time period). Moreover, transient events can generate high shear stresses between the fluid and the pipe wall. For potable water distribution systems, this may cause the resuspension of settled particles present inside the ducts, impairing the quality of the water (Boulos *et al*., 2005).

To understand how this phenomenon behaves, it is essential to take into account the risks that the water hammer can cause to the hydraulic systems, for the proper choice of the pipeline materials and the correct design of the ducts. Numerical methods are an important tool to predict the magnitudes and the frequency of the pressure waves present in the hydraulic transient. Therefore, the present work deals with the numerical solution of the conservation equations that models the water hammer phenomenon (Streeter and Wylie, 1982). These equations are solved with the finite volume method, by using a weighted-average flux total-variation diminishing (WAF-TVD) scheme (Toro, 1997).

2. METHODOLOGY

2.1 Physical Problem and Mathematical Formulation

The physical problem studied in this work was presented by Szydlowski (2002) and is schematically shown in Fig. 1.

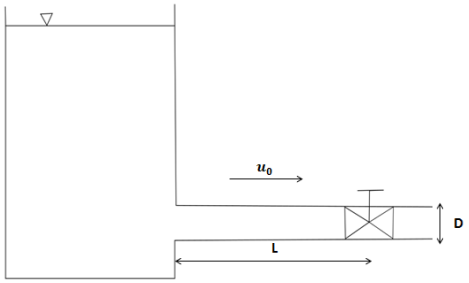

Figure 1. Configuration of the studied problem

Figure 1 shows a single horizontal steel pipe with length L and diameter D, which has a valve on one of its ends and a tank on the other end. The water initially flows from the left to the right with a velocity u_0. In a certain instant of time, the valve is closed, initiating the water hammer phenomenon, which is modeled by (Szydlowski, 2002):

$$\frac{\partial \mathbf{U}}{\partial t} + \frac{\partial \mathbf{F(U)}}{\partial x} = \mathbf{S(U)} \tag{1}$$

where

$$\mathbf{U} = \begin{pmatrix} p \\ q \end{pmatrix} \tag{2a}$$

$$\mathbf{F} = \begin{pmatrix} \dfrac{qa^2}{A} \\ Ap + \dfrac{q^2}{\rho A} \end{pmatrix} \tag{2b}$$

$$\mathbf{S} = \begin{pmatrix} 0 \\ \dfrac{-f|q|q}{2\rho AD} - f_u\left(\dfrac{\partial q}{\partial t} - a\dfrac{\partial q}{\partial x}\right) \end{pmatrix} \tag{2c}$$

In these equations, **U** is the vector of state variables, **F** is the flux and **S** is the source term, while p is the pressure, q represents the mass discharge, u is the velocity of the fluid, ρ is the fluid density, A is the cross section area of the pipe and D is the duct diameter. The parameter a is the celerity and it represents the pressure wave speed, which is given by (Szydlowski, 2002):

$$a = \sqrt{\frac{1}{\rho\left(\dfrac{1}{K} + \dfrac{D}{eE}\right)}} \tag{3}$$

where e is the thickness of the pipe wall, E is the Young's modulus of the pipe and K is the elastic modulus of the fluid.

Differently from Szydlowski (2002), we consider in the source term **S** two parameters to represent the friction between the fluid and the pipe walls. In the first term, f is the friction coefficient given by the Darcy-Weisbach formula, while the second term, f_u is the unsteady friction coefficient presented by Wylie (1997). In fact, Axworthy et al (2000) and Brunone et al. (1995) show that the use of Darcy-Weisbach formula is not valid for fast transients pipe flows, like the water hammer phenomenon.

2.2 Test cases

The verification and validation of the computational code were performed with two testes cases presented by Szydlowski (2002), as described below.

2.2.1 Test case 1

In the first test case, the pipe has 500 m of length and 0.1 m of diameter. The initial pressure value is 0.5 MPa and the initial velocity is 0.5 m/s. These values are assumed as constant in the whole pipe. At time t = 0.5 s, the valve is suddenly closed and the water hammer starts. The flow is assumed as incompressible with density ρ = 1000 kg/m^3 and the pipe wall rigid, i.e., the cross section area remains constant during the hydraulic transient. The celerity a is constant and equal to 1000 m/s. At the pipe inlet, the pressure boundary condition is prescribed as constant and equal to the initial pressure. Before the valve closure, the velocity boundary condition at the valve section is equal to the initial velocity. After the closure, the velocity at the valve section is made equal to 0 m/s.

2.2.2 Test case 2

The second test case is similar to the first, except that, now, we consider the duct elasticity and variation of the fluid density as a consequence to the water hammer. In this case, the pipeline has 72 m of length, 0.042 m of diameter and the initial velocity is 0.38 m/s. The initial pressure inside the pipe was assumed to vary linearly, from 0.51 MPa at the valve section and taking into account a friction factor based on Darcy-Weisbach formula, that is,

$$p_0 = 0.51 + f\frac{\Delta L}{D}\rho\frac{u_0^2}{2} \tag{4}$$

The boundary conditions of this case involve the imposed pressure at the pipe inlet, which was considered as the initial pressure, and the flow velocity at the valve.

The valve closure is assumed to start at time t = 0.38 s and the valve is completely closed at time t = 0.494 s. During this period that the valve is being closed, the fluid velocity at the valve section is supposed to vary from 0.38 m/s to 0 m/s linearly (Szydlowski, 2002).

Due to the sudden valve closure, pressure waves are generated in the pipe causing a change in the fluid density and a deformation of the pipe walls, according to the following equations (Szydlowski, 2002):

$$A = A_0\left(1 + \frac{D}{e}\frac{p - p_0}{E}\right) \tag{5}$$

$$\rho = \rho_0\left(1 + \frac{p - p_0}{K}\right) \tag{6}$$

where e=0.003 m, E=2x10^{11} Pa and K=2x10^9 Pa (Szydlowski, 2002).

2.3 Numerical Method

The system of equations that represents the water hammer can be split according to the following equations, in order to evolve the solution at each time step Δt, with the initial condition given by the solution at the previous time instant, i.e., $\mathbf{U}^n$ (Toro, 1997, Ozisik *et al*., 2017).

$$\left.\begin{array}{l}\dfrac{\partial \mathbf{U}}{\partial t} + \dfrac{\partial \mathbf{F(U)}}{\partial x} = 0 \\ \mathbf{U} = \mathbf{U}^n\end{array}\right\} \Rightarrow \overline{\mathbf{U}}^{n+1} \tag{7}$$

$$\left.\begin{array}{l}\dfrac{d\mathbf{U}}{dt} = \mathbf{S(U)} \\ \mathbf{U} = \overline{\mathbf{U}}^{n+1}\end{array}\right\} \Rightarrow \mathbf{U}^{n+1} \tag{8}$$

In this splitting procedure, the solution of the first system of partial differential equations is the initial condition for the second system of ordinary differential equations.

The first system was solved by the finite volume explicit method, so that we can write (Toro, 1997):

$$\mathbf{U}_i^{n+1} = \mathbf{U}_i^n + \frac{\Delta t}{\Delta x}\left(\mathbf{F}^n_{i-\frac{1}{2}} - \mathbf{F}^n_{i+\frac{1}{2}}\right) \tag{9}$$

where i is the cell position. The fluxes at the control volume surfaces are approximated by the following WAF-TVD scheme, which is written for the right volume boundary as (Toro, 1997):

$$\mathbf{F}_{i+\frac{1}{2}} = \frac{1}{2}\left(\mathbf{F}_i + \mathbf{F}_{i+1}\right) - \frac{1}{2}\sum_{k=1}^{N} sign\left(c_k\right)\phi^{(k)}_{i+\frac{1}{2}}\,\Delta\mathbf{F}^{(k)}_{i+\frac{1}{2}} \tag{10}$$

where N (=2) is the number of waves in the Riemann problem, $\phi^{(k)} = \phi^{(k)}(r^{(k)})$ is the limiter function, $sign(c_k)$ is the sign function and c_k is the Courant Number. The Courant Number for the wave speeds S_k, k = 1 and k = 2, is given by

$$c_k = \frac{\Delta t S_k}{\Delta x} \tag{11}$$

with c_0 = -1 and c_{N+1} = 1, (Toro,1997).

The flow parameter $r^{(k)}$ refers to the wave k in the solution $\mathbf{U}_{i+1/2}$ of the Riemann problem and is equal to

$$r^{(k)} = \begin{cases} \dfrac{\Delta b^{(k)}_{i-1/2}}{\Delta b^{(k)}_{i+1/2}} \text{ if } c_k > 0 \\ \dfrac{\Delta b^{(k)}_{i+3/2}}{\Delta b^{(k)}_{i+1/2}} \text{ if } c_k < 0 \end{cases} \tag{12}$$

The quantity b is a variable that changes across each wave family in the solution of the Riemann problem. In water hammer equations, this variable was set to the pressure p. In this way,

- $\Delta b^{(k)}_{i-1/2}$ denotes the jump in b across wave k in the solution $\mathbf{U}_{i-1/2}$ of the Riemann problem with data $(\mathbf{U}^n_{i-1}, \mathbf{U}^n_i)$,
- $\Delta b^{(k)}_{i+1/2}$ denotes the jump in b across wave k in the solution $\mathbf{U}_{i+1/2}$ of the Riemann problem with data $(\mathbf{U}^n_i, \mathbf{U}^n_{i+1})$
- $\Delta b^{(k)}_{i+3/2}$ denotes the jump in b across wave k in the solution $\mathbf{U}_{i+3/2}$ of the Riemann problem with data $(\mathbf{U}^n_{i+1}, \mathbf{U}^n_{i+2})$.

The limiter function $\phi^{(k)}$ provides the numerical scheme with a TVD character, in which the total variation does not increase in time. The Total Variation can be defined as (Toro, 1997):

$$TV(\xi^n) = \sum_{-\infty}^{\infty}\left|\xi^n_{i+1} - \xi^n_i\right| \tag{13}$$

where ξ is a function $\xi = \xi(x)$.

In this work, we used the Van Leer function for $\phi^{(k)}$, which has intermediate characteristics. This function is represented by (Toro, 1997):

$$\phi_{VL}\left(r, \|c\|\right) = \begin{cases} 1 & \text{if } r \le 0 \\ 1 - \dfrac{2r\left(1 - \|c\|\right)}{1 + r} & \text{if } r > 0 \end{cases} \tag{14}$$

The flux jump through the k-th wave is (Toro, 1997):

$$\Delta\mathbf{F}^{(k)}_{i+\frac{1}{2}} = \mathbf{F}^{(k+1)}_{i+\frac{1}{2}} - \mathbf{F}^{(k)}_{i+\frac{1}{2}} \tag{15}$$

where $\mathbf{F}^{(k)}_{i+1/2} = \mathbf{F}(\mathbf{U}^{(k)})$, $\mathbf{U}^{(1)} = \mathbf{U}^n_i$, $\mathbf{U}^{(2)} = \mathbf{U}^*$ and $\mathbf{U}^{(3)} = \mathbf{U}^n_{i+1}$. The vector $\mathbf{U}^*$ is calculated through the HLL method described in Toro (1997). In this method, the vector $\mathbf{U}^*$ is given by

$$\mathbf{U}^* = \mathbf{U}^{hll} = \frac{S_R\mathbf{U}_R - S_L\mathbf{U}_L + \mathbf{F}_L - \mathbf{F}_R}{S_R - S_L} \tag{16}$$

where S_L and S_R are two wave velocities, which can be taken as (Toro, 1997):

$$S_L = \min\left\{\lambda_1^L, \lambda_1^R\right\} \tag{17a}$$

$$S_R = \min\left\{\lambda_2^L, \lambda_2^R\right\} \tag{17b}$$

where $\{\lambda_1{}^L, \lambda_1{}^R\}$ and $\{\lambda_2{}^L, \lambda_2{}^R\}$ are the eigenvalues $\lambda_1 = u - (u^2+a^2)^{1/2}$ and $\lambda_2 = u + (u^2+a^2)^{1/2}$ of the following Jacobian matrix for the cells i and i+1

$$\mathbf{J} \equiv \frac{\partial \mathbf{F}}{\partial \mathbf{U}} = \begin{pmatrix} \dfrac{\partial F_1}{\partial U_1} & \dfrac{\partial F_1}{\partial U_2} \\ \dfrac{\partial F_2}{\partial U_1} & \dfrac{\partial F_2}{\partial U_2} \end{pmatrix} = \begin{pmatrix} 0 & \dfrac{a^2}{A} \\ A & \dfrac{2q}{\rho A} \end{pmatrix} \tag{18}$$

Numerical boundary conditions were used in this work for fictitious volumes. For i = 1 and i = M cells. Laney (1998) shows an extrapolation technique using two fictitious volumes for the left and right boundaries as:

$$\mathbf{U}_0^n = \mathbf{U}_1^n \tag{19a}$$

$$\mathbf{U}_{-1}^n = \mathbf{U}_2^n \tag{19b}$$

$$\mathbf{U}_{M+1}^n = \mathbf{U}_M^n \tag{19c}$$

$$\mathbf{U}_{M+2}^n = \mathbf{U}_{M-1}^n \tag{19d}$$

where i = -1 and i = 0 are the fictitious volumes at the inlet and i = M+1 and i = M+2 are the fictitious volumes at the outlet. In this way, the numerical method is applied for all i cells, for i=1, 2, …, M-1, M. At the pipe inlet, pressure is prescribed and mass discharge is extrapolated, while, at the outlet, mass discharge is prescribed and pressure is extrapolated.

The solution of Eq. (9) with the WAF TVD scheme allows us to solve Eq. (10). This system of equations was numerically integrated by using the following explicit finite difference scheme:

$$\mathbf{U}_i^{n+1} = \overline{\mathbf{U}}_i^n + \mathbf{S}(\mathbf{U}^n)\Delta t \tag{20}$$

3. RESULTS

3.1 Test Case 1

The analytical solution for the pressure variation at the valve section is present in Szydlowski (2002) and is shown in Fig. 2.

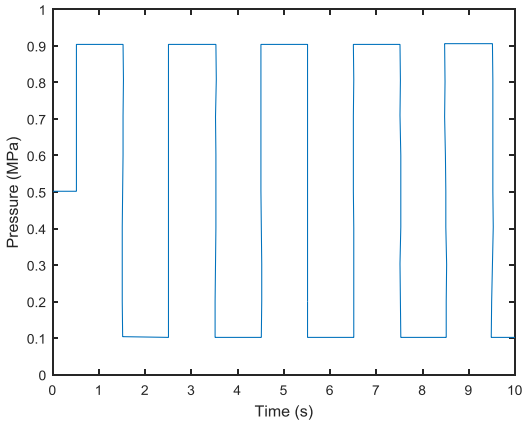

Figure 2. Analytical Solution for Test Case 1 (adapted from Szydlowski, 2002).

To verify the numerical solution given by the WAF-TVD scheme, a grid convergence analysis was performed to select the number of finite control volumes. We can see in Fig. 3 the graphic convergence between the results using 500 and 1000 control volumes and our numerical solution with 500 control volumes agrees relatively well with the analytical solution, as presented by Fig. 4.

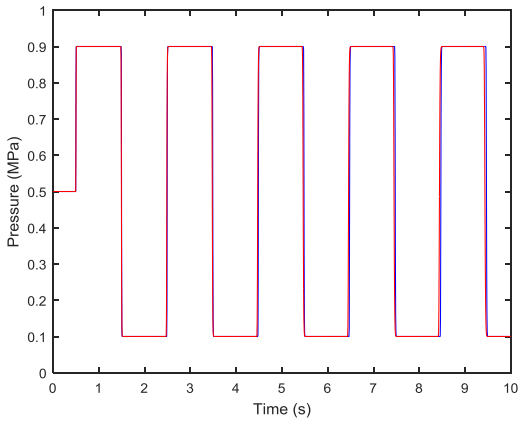

Figure 3. Comparison between the numerical results using 500 control volumes (red line) and 1000 control volumes (blue line)

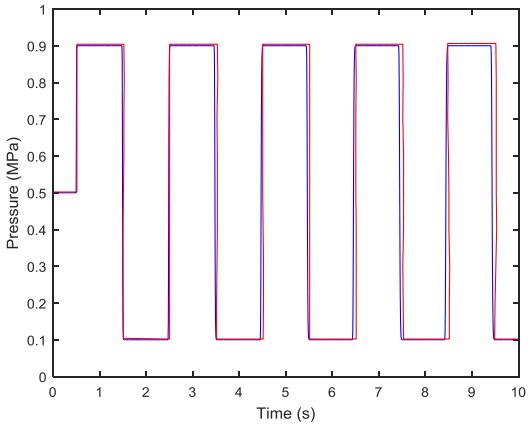

Figure 4. Comparison between the numerical results using 500 control volumes (red line) and the analytical solution (blue line)

Figure 4 shows that the numerical method was capable of retrieving the same pressure waves magnitudes given by the analytical solution, as well the frequency of these waves. A little disagreement can be seen from t = 8s until t = 10 s. This fact could be caused by inaccuracies in the graphical procedure used to obtain the analytical data from the curves presented by Szydlowski (2002).

3.2 Test Case 2

For the numerical solution of this second case, the friction term given by Wylie (1997) is needed. In this term, the unsteady friction factor was arbitrarily set to f_u=0.0433 and the two derivatives were approximated by finite differences. For the time derivative, backward finite differences of first order were used for all control volumes. For the spatial derivative, central finite differences of forth order were used for the central control volumes and, at the boundaries, the backward and forward finite differences of forth order were used in the pipe inlet and at the valve section, respectively.

For the grid convergence analysis, the numerical results for the pressure variation at the valve section using 500, 1000 and 2000 control volumes were examined. This analysis was done graphically and numerically. Figure 5 shows that the graphic convergence was obtained for all three solutions.

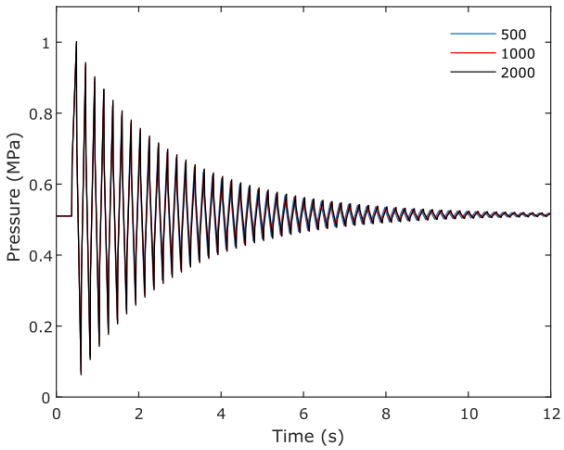

Figure 5. Numerical results using 500, 1000 and 2000 control volumes

The pressure values and times for selected peaks were compared for the numerical solution obtained with different numbers of control volumes. These results are presented by Tables 1 and 2, for the time values and pressure values, respectively.

Table 1. Time values (s) for 500, 1000 and 2000 control volumes

	Number of Control Volumes		
Peak Order	500 volumes	1000 volumes	2000 volumes
1	0.4884	0.4894	0.4900
5	0.9279	0.9309	0.9326
9	1.3680	1.3730	1.3760
13	1.8080	1.8150	1.8190
17	2.2440	2.2570	2.2620
21	2.6890	2.7000	2.7050
25	3.1300	3.1420	3.1428
29	3.5700	3.5840	3.5920
33	4.0110	4.0270	4.0350
37	4.4520	4.4690	4.4780

Table 2. Pressure values (MPa) for 500, 1000 and 2000 control volumes

	Number of Control Volumes		
Peak Order	500 volumes	1000 volumes	2000 volumes
1	0.9969	1.0010	1.0030
5	0.8898	0.8988	0.9042
9	0.8226	0.8313	0.8367
13	0.7688	0.7769	0.7819
17	0.7252	0.7325	0.7370
21	0.6895	0.6959	0.7000
25	0.6601	0.6658	0.6694
29	0.6358	0.6408	0.6440
33	0.6157	0.6201	0.6229
37	0.5990	0.6027	0.6052

An analysis of Tables 1 and 2 reveals that the numerical values for the time and pressure at each pressure peak are very close, for the different numbers of control volumes used. The same conclusion can be obtained from the analysis of the relative percentage deviation between the numerical solutions using 500 and 2000 control volumes, as well as 1000 and 2000 control volumes, which are presented by Tables 3 and 4, for the time and pressure values, respectively.

Table 3. Relative percentage deviation for the time values in relation to the numerical solution of 2000 control volumes

	Number of Control Volumes	
Peak Order	500 volumes	1000 volumes
1	0.3	0.1
5	0.5	0.2
9	0.6	0.2
13	0.6	0.2
17	0.8	0.2
21	0.6	0.2
25	0.4	0.2
29	0.6	0.2
33	0.6	0.2
37	0.6	0.2

Table 4. Relative percentage deviation for the pressure values in relation to the numerical solution of 2000 control volumes

	Number of Control Volumes	
Peak Order	500 volumes	1000 volumes
1	0.6	0.2
5	1.6	0.6
9	1.7	0.7
13	1.7	0.6
17	1.6	0.6
21	1.5	0.6
25	1.4	0.5
29	1.3	0.5
33	1.2	0.5
37	1.0	0.4

Table 3 shows that the relative deviation for the time values is less than 1%, showing an excellent agreement grid convergence. Although the maximum pressure relative differences between the results obtained with 500 and 2000 control volumes (see Table 4) are of 1.7%, this difference becomes smaller than 1% between the results obtained with 1000 and 2000 control volumes. Therefore, for the results presented below, 1000 control volumes were used for the numerical solution based on the WAF-TVD method described above.

The numerical solution obtained with 1000 control volumes is presented in Fig.6 and is compared with Fig. 7 that shows the experimental results for the pressure variation at the valve section (Szydlowski, 2002).

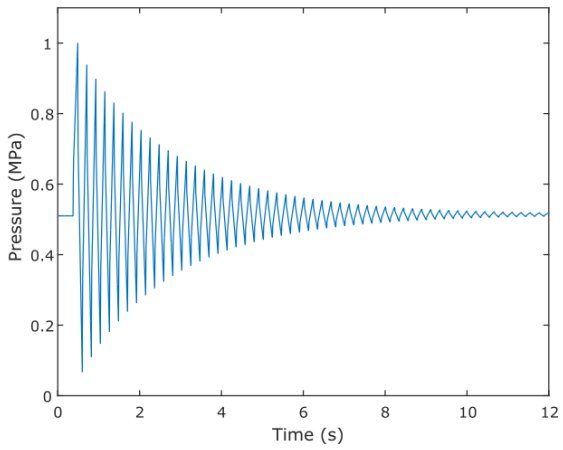

Figure 6. Numerical Results using 1000 control volumes

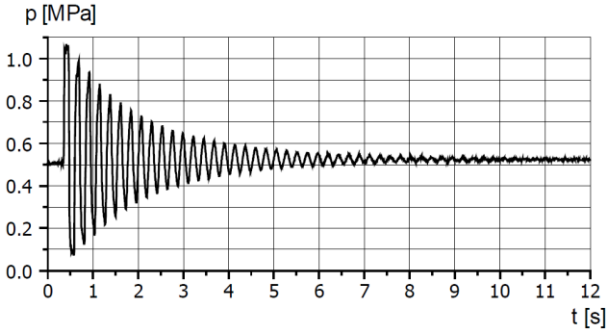

Figure 7. Experimental results for test case 2.

Figures 6 and 7 show a very good agreement between numerical and experimental results. The shape of the numerical curve was very similar to the measurements and the pressures waves with lager magnitudes were accurately predicted. The magnitude of damped waves was slightly larger for the numerical solution. This fact can be explained by the chosen model presented by Wylie (1993) and the arbitrarily value of 0.0433 chosen for the unsteady friction factor f_u. The use of another friction model or another friction factor value might still improve the results.

4. CONCLUSIONS

The main goal of this work was the numerical implementation of the WAF-TVD scheme to solve water hammer equations. For the verification and validation of the computational code, the numerical solution was compared with two test cases present in the literature. In the first case, the water hammer takes place in a frictionless duct where the cross section area and the fluid density do not vary. For this case, it was observed that the numerical solution with 500 control volumes produces a result very close to the analytical solution.

The second test case analyzed deals with friction at the pipe walls and the variation of the cross section area and fluid density as a consequence of the hydraulic transient. It was seen through a grid convergence that the numerical solution using 1000 volumes was appropriate for this test case. Comparing the experimental solution presented in Szydlowski (2002) and the numerical solution, we observed a very close agreement between them. Some discrepancy was observed, however, this can be explained by the friction model given by Wylie (1993).

Thus, we conclude that the WAF-TVD scheme can be a very powerful tool to solve the water hammer equations and can be used to predict the behavior of the pressure waves generated in this phenomenon.

5. REFERENCES

Axworthy, D. H., Ghidaoui, M. S., Mcinnis, D. A., *Extended Thermodynamics Derivation of Energy Dissipation in Unsteady Pipe Flow*, Journal of Hydraulic Engineering, vol. 126(4), pp. 276-287, 2000.

Boulos, P. F., Karney, B. W., Wood, D. J., Lingireddy, S, *Hydraulic Transient Guideless for Protecting Water Distribution Systems*, Journal of American Water Association, pp.111-124, 2005.

Brunone, B., Golia, U.M., Greco, M., *Effects of Two-Dimensionality on Pipe Transients Modeling*, Journal of Hydraulic Engineering, vol. 121 (12), pp. 906-912, 1995.

Laney, C. B., *Computational Gasdynamics*, Cambridge, Cambridge University Press, 1998.

Lüdecke, H. J., Kothe, B., *KSB Know- how Water Hammer*, Volume 1, KSB, 2006.

Ozisik, N., Orlande, H. R. B., Colaço, M. J., Cotta, R. M., *Finite Difference Methods in Heat Transfer*, 2ª Ed., CRC Press, 2017.

Streeter, V. L., Wylie, E. B., *Mecânica dos Fluidos*, 7ª Ed., Editora McGraw-Hill do Brasil, 1982.

Szydlowski, M., *Finite Volume Method for Water Hammer Simulation*, I International Scientific and Technical Conference on Technology, Automation and Control of Wastewater and Drinking Water Systems, TiASWiK'02, pp. 159-165, 2002.

Toro, E. F., *Riemann Solvers and Numerical Methods for Fluid Dynamics*, 2ª ed. Berlin, Springer, 1997.

Wylie, E. B., *Frictional effects in unsteady turbulent pipe flows*, Applied Mechanics Reviews, Vol. 50, nº 11, pp. 241-244, 1997.

6. RESPONSIBILITY NOTICE

The authors are the only responsible for the printed material included in this paper.